Impact of Inkjet Printing Parameters and Environmental Conditions on Formation of 2D and 3D Binder Jetting Geometries

Trenton Colton, Colton Inkley, Adam Berry, Nathan B. Crane
Mechanical Engineering Department, Brigham Young University, Provo, UT

Abstract

While Binder Jet Additive Manufacturing (BJAM) has great potential, its implementation is limited by defects in the finished parts. An improved understanding of how printing parameters impact the quality of the printed parts is needed. Prior work on the droplet/powder interactions in BJAM printing focused on individual lines, this work shows that successful layer formation favors larger droplet spacing than is viable in individual lines. When printing layers, the first printed layer was significantly rougher than the spread bed indicating significant powder ejection. However, this difference was eliminated after printing 1-4 additional layers. These results show that prior printed layers have a strong impact on droplet impact and imbibition and that simple droplet or line geometries are not effective for testing printing parameters. The roughness of the first layer may contribute to large pores observed between layers. This paper further examines the impact of key printing parameters including layer thickness, droplet/line spacing, and droplet inter-arrival time on the effective saturation and surface roughness of 2D and 3D parts. The droplet inter-arrival time (print frequency) had negligible impact on surface roughness and saturation under the conditions tested. Printed layers behaved similarly at droplet spacing values comparable to the droplet diameter (44 μm). In contrast, droplet spacing of 60 μm, produced substantially lower saturation. Effective saturation generally increases with increased number of layers. Ambient humidity exposure during printing is shown to have a negligible impact on printing outcomes though higher moisture levels from steam exposure dramatically alter saturation. Drying powder before spreading reduced variation in the printed parts. All tests were based on gas atomized -22 μm 316 SS powder.

INTRODUCTION

Binder jetting (BJ) is an additive manufacturing (AM) process that uses inkjet technology to deposit a binding agent on thin layers of powder. The binding agent binds the powder within the cross section of each layer and between layers. As demand for AM has grown and early BJ patents have expired, interest in BJ has increased in both academia and industry [1]. BJ offers potential for lower costs and higher build rates compared to other AM methods due to use of inkjet technology for rapid patterning. Unlike AM processes that require high energy input for fusion (i.e., direct energy deposition, laser powder bed fusion), relatively little heat is applied in BJ. In addition, no support structures are required. BJ can print any powdered material including ceramics [2], metals [3], and polymers [4]. This flexibility has driven BJ use in biomedical, foundry, automotive, and aerospace industries [5].

However, compared to other additive manufacturing processes, industrial adoption of BJ for production has been slower due to reduced properties and post-processing challenges. The properties are often limited by residual porosity after post-processing. While liquid phase sintering has greatly improved densification of the green parts [6-8], large pores that are introduced during the printing process are difficult to eliminate. The source of these large pores needs to be better understood so that their formation can be prevented. Neither the mechanisms for formation of large pores nor the relationships between printing parameters and surface roughness are understood.

Most studies of printed parts use commercial equipment that does not provide much control over key parameters such as droplet velocity, droplet volume, droplet spacing, droplet inter-arrival time, and line spacing [9-12]. Parameters such as droplet velocity are not readily measured on these machines and the droplet placement patterns may be unknown.

There is also need for improved understanding of print saturation—the key user-selected printing parameter on commercial equipment. Saturation is selected by printing test parts and inspecting them to determine the quantity of binder to be deposited (target saturation level) to avoid bleeding for each specific powder, binder, printhead, and machine [10, 13-16]. Acceptable saturation levels can be impacted by drying parameters as well [17]. While general trends for the impact of parameters such as printing speed [13], in-process drying [17, 18] and layer thickness [19, 20] have been noted, significant testing is still required to select parameters for new printing conditions and materials.

During printing, picoliter-scale droplets of binder impact the powder bed to form lines as the printhead moves over the bed. Adjacent nozzles in commercial printheads are typically farther apart than the diameter of the line formed by adjacent droplets so additional printheads or repeated passes with a single printhead are required to fill in the gaps between lines. As printing proceeds, adjacent lines merge to become part layers. Following binder deposition, the surface is often heated to partially evaporate the solvent from the binder. A new layer is spread, and this process is repeated layer-by-layer until the full part is built. The resultant "green" part consists of powder particles held together with binder. Green parts are fragile and are usually post processed by sintering and/or infiltration to improve mechanical properties [21, 22].

Relatively little is known about how inkjet droplets interact with powder. Primitives of single mm-scale droplets in powder have been used to study granulation [23-25], but the droplet volumes in these studies (microliters) are orders of magnitude larger than those typically used in BJ (picoliters). In addition, these studies do not include interaction between new droplets and previous droplets even though moisture in the powder significantly changes the wetting and infiltration behavior [26].

More studies have been done of t droplets deposited close together to form lines. High speed optical and x-ray imaging of line printing showed that the binder/powder interaction causes particle ejection and powder bed deformation which densify some powder regions while creating pores in others [27, 28]. Seluga [29] and Colton [30] showed that increasing droplet velocity improves line formation but also alters the effective saturation (discussed further below). The magnitude of these effects depends on droplet size and the square root of the droplet inter-arrival time. Line formation (the ability for droplets to coalesce into a continuous line) also depends on droplet size/spacing and droplet inter-arrival time (frequency) [19, 30, 31]. Recent studies of printed lines [32], show that at low droplet velocity (2.4 m/s), small droplet spacing (high droplet overlap) or long droplet interarrival times is required for successful formation of uniform lines in the powder [32]. However, these printing conditions are not desirable for BJ because they create large line diameters. The line diameter limits the minimum feature size while the long inter-arrival time limits the printing speed. This is perhaps the reason that small droplet spacing is not seen in commercial systems. Instead droplet spacing is commonly comparable to the droplet size [19, 29]—a condition that did not successfully form lines in a prior study [32].

To improve the implementation of BJ in industry, the fundamental binder/powder interaction must be understood further. To facilitate this understanding, this paper seeks to extend

studies based on droplets and lines to single and multiple layer parts since most part geometry is composed of multiple layers of adjacent lines. Binder, powder, and printing conditions from prior studies of line printing are used for comparison [32]. Little is known about the applicability of studying primitives such as individual droplets or lines to understand the printing of 3D parts. The results show that line and primitive tests should be replaced by layer testing because line results do not accurately predict the feasible printing parameters, saturation, or surface roughness of printed layers.

This paper also advances the understanding of the relationships between printing parameters and printing outcomes of saturation and surface roughness. These are relevant because print saturation is a key process parameter that must be selected by the user while the surface roughness provides an indication of powder rearrangement during printing. Powder rearrangement may contribute to large pore formation, reduced green part density, and poor appearance of the part surfaces. The dependence of saturation and roughness on printing parameters (droplet/line spacing, droplet frequency, and layer thickness) are measured for parts made of 1, 2, 3, and 5 layers. Additionally, the powder is exposed to environmental conditions (humidity, steam) and powder conditioning (drying) to assess the sensitivity of the printing parameters to powder conditioning and ambient printing conditions. These measurements provide insight into selection of printing parameters and the need for powder conditioning and/or environmental control during printing. This study focuses on commercially relevant combinations of droplet size, droplet spacing, and layer thickness with a -22 μm 316 SS powder.

SATURATION

One parameter that represents key aspects of the binder/powder interaction is binder saturation. In BJ, saturation is defined as the percentage of void space in the powder bed filled with binder and "print saturation" is a target value of saturation set by the user. If binder remains in the intended region, the print saturation is given by

$$S_p = \frac{\pi\, D_d^3}{6\, \Delta x\, \Delta y\, \Delta z\left(1 - P_f\right)} \tag{1}$$

where S_p is print saturation, D_d is the diameter of the binder droplet, Δx is droplet spacing, Δy is line spacing, Δz is layer thickness, and P_f is packing fraction of the powder bed. Packing fraction is the ratio of powder bed density to full material density. In commercial systems, the user typically inputs the packing fraction (P_f) and specifies the target print saturation (S_p) and layer thickness (Δz). The machine software then selects the droplet and line spacing based on proprietary algorithms to deposit the targeted amount of binder/volume of part. However, the binder may fill more or less space than targeted due to variables including powder/binder wetting properties, printing parameters, and drying conditions [17]. This will cause the actual effective saturation (S_e) to differ from the target value. The value of S_e can be calculated from the part weight as

$$S_e = \frac{m_b \rho_{pb}}{m_p \rho_b * (1 - P_f)} \tag{2}$$

where m_b is the mass of the deposited binder, $\rho_b$is binder density, m_p is the mass of the bound powder, ρ_{pb} is powder bed density, and $P_f$is the packing fraction.

Single printed lines typically have much lower effective saturation (S_e) levels than the print saturation [30]. When adjacent lines and subsequent layers are printed, binder must connect to previously wetted regions to assure that the entire part is bound together. If saturation is too high and exceeds the stable limits, binder will migrate outside the predetermined space producing a defect commonly known as "bleeding." Bleeding negatively impacts part dimensional accuracy. Some extra binder beyond the line saturation limit can be accommodated because (1) hysteresis in powder wetting (discussed below), and (2) binders typically contain volatile solvents. Some solvent from the printed binder evaporates leaving space to absorb excess binder in a new layer. Most commercial processes incorporate heating between layers to increase evaporation. Prior work has shown that this drying is critical to increasing the saturation range that generates accurate parts [17].

While a user selects a single target print saturation, the printing process usually creates a range of saturation values in the part that vary both spatially and temporally due to hysteresis in the imbibition and drainage curves [33]. As droplets impact the surface, the powder region near the impact region saturates with binder. Capillary pressure drives fluid to the surrounding partially saturated and unsaturated regions until the pressure is equilibrated across the fluid network. While the capillary pressure equilibrates, the saturation can vary spatially due to hysteresis between drainage and imbibition curves However, due to the measurement challenges, this spatial variation has not been characterized. The target print saturation is typically reported and only an effective saturation (S_e) averaged over a part is typically measured [14, 16, 34].

Equilibrium saturation is the maximum print saturation where the binder will not flow past the desired boundaries. Methods of predicting equilibrium saturation levels have been proposed. Miyanaji, et.al [35] developed the first physics based equilibrium saturation model based on a single equivalent pore size. Unfortunately, limited experimental data did not correlate with predicted values. Dynamic contact angle [36], in-process drying [17], droplet velocity and size [30] have all been shown to alter part saturation values suggesting that this quantity is a function of the process parameters and not the powder and binder alone.

METHODS

Materials

ExOne solvent binder was used in each of the experiments conducted. Binder properties as provided by the manufacturer are density 1.05 g/cc, viscosity 4.6 cps, surface tension 32 dynes/cm. All experiments used ExOne 316 stainless steel powder (D_{50} = 10 μm). Particle size distribution was measured using laser diffraction by NSL analytical (ISO 13320). Particle shapes were observed using scanning electron microscope (Apreao C SEM). Particle distributions and SEM images are shown in Figure 1.

Powder Conditioning Procedures

Moisture can impact the binder jetting process in two phases. First, moisture absorption during storage from the ambient environment would tend to decrease the packing density by increasing the cohesion of the powder bed [37, 38]. Secondly, moisture in the powder during printing is expected to accelerate binder imbibition [26] and may reduce powder ejection by increasing cohesive strength [39]. To separate the impact of ambient humidity levels on the spreading and printing phases, the humidity exposure of the powder before and after the printing process was varied. The surface roughness and effective saturation of the resulting parts was measured under each condition. Four powder conditions were used: 1) powder treated with

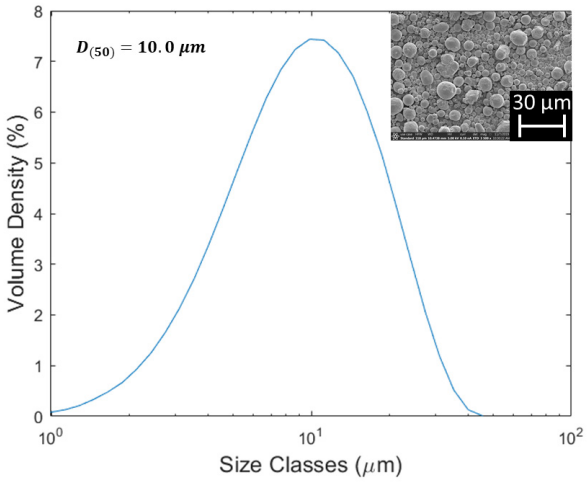

Figure 1: Particle size distribution and SEM images for the 316 SS powder used in experiments.

ambient humidity exposure printed at ambient conditions (Amb-Amb); 2) dried powder exposed to 40% humidity before printing (Dry-40%); 3) dried powder exposed to 80% humidity before printing (Dry-80%); and 4) dried powder exposed to steam for 10 s before printing (Dry-Steam). This helps provide insight into the relative impact of powder conditioning before printing (dry or ambient humidity exposure) to the impact of humidity exposure during the layer spreading and printing process itself.

Dry powder was prepared by heating the powder for 8 hours at 180° C and then storing in airtight containers until use. Powder with ambient moisture was obtained by first drying the powder and then exposing it to ambient humidity (≈30%) for 48 hours before printing. During printing, a small amount was removed to be spread for each layer. Humidity exposure during printing (40% and 80%) was achieved by enclosing the apparatus and controlling the humidity levels in the chamber. To maximize the impact of elevated humidity exposure, each layer in the experiments with high humidity conditions was exposed to the controlled environment for 10 minutes between spreading and printing. Steam exposure for 10 s from a household steamer was used to imitate extremely moist environments. After dried powder was spread, the steam source was held about 18 inches from the powder bed surface to not disturb the bed and steamed for 10 seconds at each layer prior to printing. During steam tests, the humidity chamber was maintained at 80% saturation to reduce evaporation from the powder bed after steam application.

Droplet Characterization

Droplet volume remained constant between tests and was measured by printing at constant frequency for two minutes while capturing the droplets in a small container. The droplets were weighed to calculate the weight of a single droplet (45 pl, diameter ~44 µm). Images produced from IDS UI-3370CP-M-GL camera at 2.5x magnification and a strobing LED behind the droplets were used to measure droplet velocity. Each droplet velocity data point is the average of six samples.

Powder Bed Density Measurements

The average of at least three measurements was used for each condition. Powder bed density was measured by using the plug method in which a sample of powder is extracted by

inserting a cylindrical plug of a known size (2.8 cm diameter) into the powder bed and weighing the powder [40]. Powder bed density was 4.35 g/cm³ (55% packing fraction). Repeated measurements of density fell within 1% of the target packing fraction for all powder conditions.

Part Fabrication

All experiments were printed using a custom-built binder jetting apparatus. The apparatus consisted of a single MicroFab MJ-AB printhead (30 μm orifice), Techno DaVinci CNC router modified with a Gecko G540 controller, and a custom powder spreader. All were controlled using a LabVIEW VI and a NI cRio device. All tests were conducted at an ambient temperature of 21°C. The apparatus was enclosed in a chamber with humidifiers controlled with an Inkbird IHC-200 humidity controller. Humidity levels were logged with an additional humidity sensor (Omega OM-HL-SP-TH). To separate the impact of printing parameters from drying, the powder bed was not heated during printing or between layers.

Two types of parts were printed: single 10 mm lines, and layers. Arrays of single lines of 10 mm length were printed on beds of spread powder with a spacing of at least *** between adjacent lines. A minimum of *** lines were printed for each printing condition. Lines were printed with a range of droplet velocities by varying the droplet waveform.

Layer parts were fabricated as 10 mm x 7.5 mm rectangles. Thicknesses varied based on the number of layers printed (1, 2, 3, 5, 8). Layer thickness values of 35, 50, and 65 μm were utilized. Droplet velocity remained constant for all printed layers at 4.9 m/s. The layer tests reported in this paper are based on droplet spacing values selected to be comparable to the droplet diameter (44 μm) as is commonly practiced in commercial instruments. Droplet spacing and droplet frequency were varied in the experiments with values of 40, 50, 60 μm and 500 and 1000 Hz respectively. Line spacing was equal to droplet spacing for all layer printing tests.

After printing each set of parts, the powder bed was heated at 180°C for 1 hour. After air cooling, surface roughness was measured on the printed surface of two to three parts from each parameter set using a 3D profilometer (Zeta 20). Parts were then extracted and cleaned using pressurized air through an 18-gauge needle. The extracted parts were weighed, and their effective saturation calculated using Eqn. (2).

Part Cross-sectioning

Selected parts printed in 316 SS were cross sectioned to look for large pores. To minimize disruption of the green parts during sectioning, they were first infiltrated with cyanoacrylate adhesive to increase strength and cured in air. Low viscosity clear epoxy was then infiltrated under vacuum for 8 hours. This improved infiltration and decreased porosity in the epoxy. Parts were mounted in polishing epoxy following infiltration. Surfaces were then sectioned, polished, and imaged using an Olympus GX51 microscope.

RESULTS AND DISCUSSION

The experiments described above are considered in three main groups. First, the formation of lines and layers under similar printing conditions are compared to elucidate the limitations of using simplified geometries for studying printing parameters. Then the impact of printing parameters on the surface roughness is examined. Increases in surface roughness from printing indicate the level of powder rearrangement during printing. Next, the impact of printing parameters on effective saturation in parts with varying number of layers is observed. These results provide valuable insight into the selection of saturation for parts of varying thickness and the suitability of

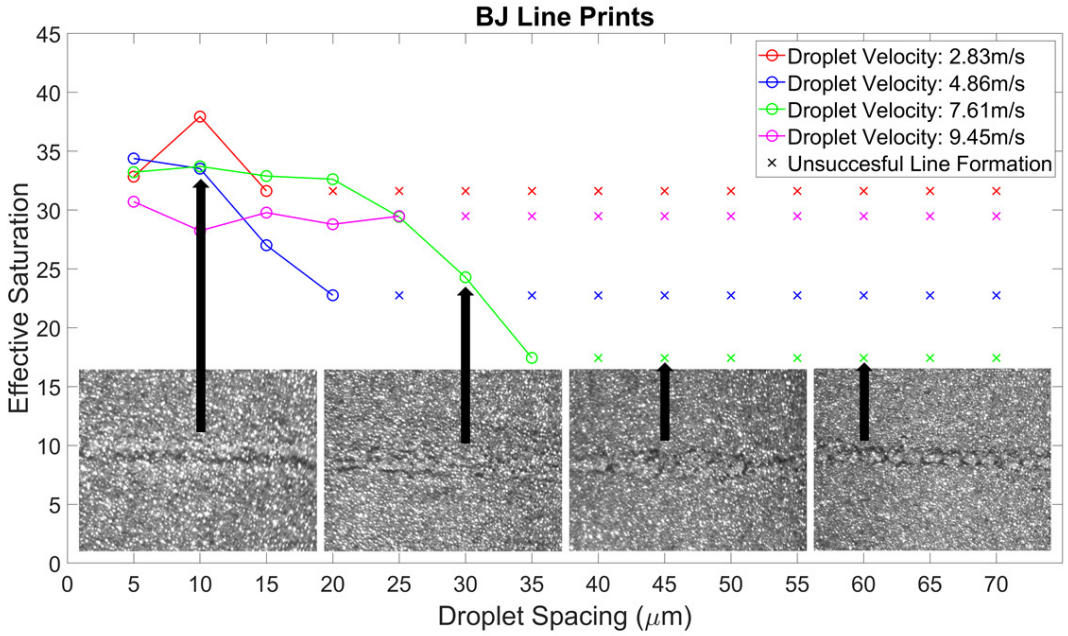

Figure 2: The saturation results of printed lines at different combinations of droplet velocity and spacing with a constant droplet generation frequency of 1 kHz. Data stops when less than 60% of lines could be extracted. Saturation is calculated from the combined weight of 5 printed lines.

using a single saturation value for all values of droplet spacing and layer thickness. Finally, the impact of powder drying and ambient conditions during printing on both saturation and surface roughness are considered.

Comparison of Line and Layer Printing Parameters

In previous work [32], successful line formation in the 316 stainless steel powder was shown to be favored by spaces between droplets that were much smaller than the droplet diameter. The largest droplet spacings were achieved with longer times between droplet arrivals (lower printing frequency). This prior dataset was expanded to assess the impact of velocity on formation of lines and saturation as summarized in Figure 2. From droplet velocity of 2.83 m/s to 7.61 m/s, increasing droplet velocity allowed lines to successfully form at larger droplet spacings. The highest velocity of 9.45 m/s did not follow this trend—possibly due to increased powder ejection or splashing. However, all printing conditions generated broken segments and balling before the droplet spacing was comparable to the droplet size (44 μm). No printing velocity formed lines above 35 μm droplet spacings.

To test the applicability of the line-printing conditions to layer printing, layers were printed using a raster pattern at a droplet frequency of 1 kHz, droplet velocity of 4.9 m/s, and droplet spacing values of 5, 7.5, 10 μm with line spacing values from 110-440 μm for a total of 24 different combinations. All tests were conducted using powder exposed to ambient moisture and printed under ambient conditions (Amb-Amb). While these conditions successfully formed lines [30, 32], layers printed under these conditions failed to merge at larger line spacings or experienced significant bleeding with notably thicker parts on the region that was printed first. In addition to the low quality of the resulting parts, these small droplet spacing printing conditions are also

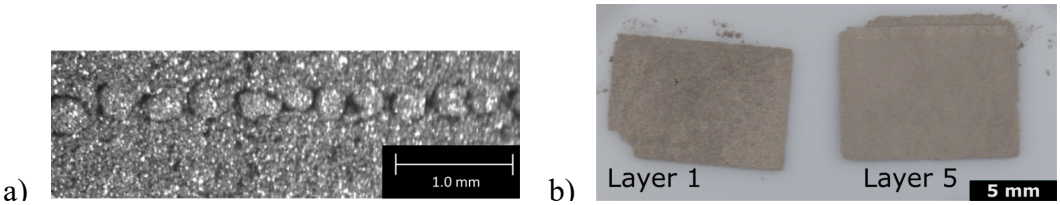

Figure 3:Comparison of lines and layers printed under the same conditions a) Balling seen in line printing. b) Layers printed under the same conditions from continuous parts that can be extracted. Print parameters were 1 kHz droplet frequency, 4.9 m/s droplet velocity, and 50 µm droplet spacing.

undesirable as the closely spaced droplets create large features that reduce the process resolution. In contrast, droplet spacings (40-60 µm) comparable to the droplet diameters (44 µm) broke up into smaller balls or segments rather than form continuous lines as seen in Figure 2 and Figure 3a, but did form layers consistently as seen in Figure 3b and detailed in subsequent sections.

This success in layer formation where lines do not form suggests that interactions of newly arriving droplets with adjacent previously printed lines may play a crucial role in preventing balling. These results show that conditions for successful line and layer printing can be very different and that it is preferable to study 2D and 3D geometries (layers and multilayers) rather than 1D lines to understand the printing parameters. However, where maximum feature resolution is desired, the formation of individual lines may be relevant.

Surface Roughness

Layers were printed with equal spacing between droplets and adjacent lines. Printing a single part layer significantly increases the surface roughness (Sa) from an as-spread value of 8.6 to 10-13.5 µm as seen in Figure 4. The increased roughness of the printed surface is caused by powder motion during printing either due to ejection or balling. Powder motion is likely to reduce the density of the green part below the initial powder bed density (often >60%). This increases shrinkage and/or porosity in the final part. However, after printing additional layers, the surface roughness of the succeeding layers decreases back to the as-spread level. Optical measurements of surface roughness (Figure 5) confirm this visual observation across the wide range of printing

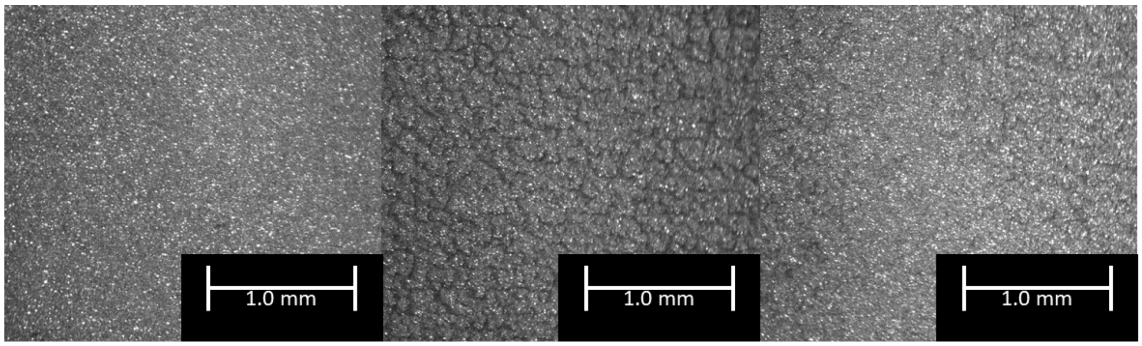

Figure 4: (Left) Bare powder bed imaged prior to printing. (Middle) First layer of 316 SS surface at 5x magnification aspects similar to balling defects from line printing can be seen, a relatively rough surface. (Right) Third layer of 316 SS at 5x magnification, a smoother surface is seen. Both were printed at 50 µm layer thickness, droplet spacing, and line spacing. Print saturation was approximately 90%.

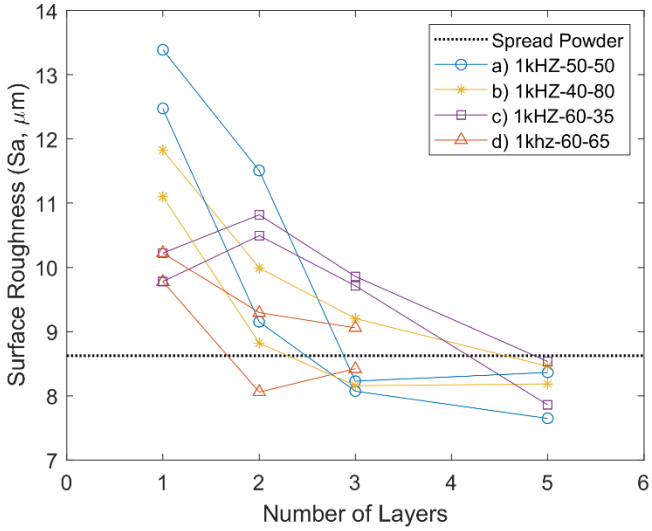

Figure 5: Surface roughness values of single- and multi-layer parts printed in ambient moisture powder. Each condition was sampled two times. Legend depicts print parameters in order: droplet frequency-droplet spacing (μm)-layer thickness (μm).

conditions tested. The printed surface is typically smoother than an un-printed powder bed after printing three to five layers though it was achieved as quickly as the second layer in one test.

The printing conditions (a-c) in Figure 5 produce the same approximate target saturation level of 88-90%. Since the droplet size was fixed, the layer thickness was varied to compensate for changes in droplet and line spacing. However, the layer thickness does not play a role in the first printed layer as seen by comparing the first layer outcomes for printing condition 'c' and 'd' in Figure 5. The roughness of the first printed layer was smallest at the largest droplet spacing of 60 μm. At this larger spacing, the 44 μm droplets are unlikely to interact before penetrating the powder bed. Despite the larger droplet spacing, all the printed surfaces had sufficient strength to be removed from the powder bed for saturation measurement (discussed below). This indicates that the binder formed a continuous network within the powder after imbibition. The surface roughness after printing seems to be due, at least partially, to some balling effects (Figure 4) of printing at droplet spacing comparable to droplet diameters though powder ejection may also be significant as seen in [27].

The declining roughness of subsequent printed layers seen in Figure 5 may be explained by a change in the droplet imbibition or powder mechanics when printing over a layer of moist powder. The reduced roughness may be explained by a significant decrease in powder ejection when printing over previously printed layers. This observation suggests that measurements of single line [27] or even single layer printing provide limited insight into the formation of the bulk part geometry. Since the number of layers impacts surface roughness across all printing conditions, the interaction between layers must play a substantial role in affecting BJ parts at least comparable to the interaction between droplets of the same layer. Surprisingly, among the samples with ~90% print saturation, the samples with larger layer thicknesses returned to the initial surface roughness levels more rapidly. Condition 'c' with 60 μm droplet/line spacing and the smallest layer spacing (35 μm) had higher roughness in the second layer than the first. When the layer thickness was increased to 65 μm the same droplet line spacing showed similar rate of smoothing

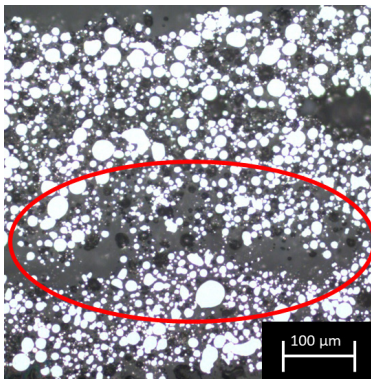

Figure 6 Cross section of a 5-layer part. Large porosity seen between first and second layer

as conditions 'a' and 'b'. While both droplet/line spacing and layer thickness impact the initial roughness and the change with subsequent layers, these observations demonstrate that layers can be formed successfully over a wide range of printing conditions (layer thickness, saturation, droplet spacing) and that some problems in printing an initial layer can be overcome when printing subsequent layers

However, that does not mean that all printing conditions will provide equal part quality. If powder from the newly spread layer does not completely fill the crevices in the rough surfaces of the first layer or if balls of binder remain on the surface while spreading the next powder layer, the surface roughness seen on the first layers could be a source of defects as layers are stacked and bonded together to form a part. To evaluate for large pores, parts were infiltrated with epoxy and sectioned. Of the samples sectioned, many had large pores just above the first layer as seen in Figure 6. Furthermore, no such defects were found near the last layers of the parts that were sectioned. These defects are reminiscent of large pores parallel to the layers documented in prior studies [41]. It is possible that surface roughness after printing could be one mechanism for forming these pores. This is important as the largest pores are most difficult to eliminate by sintering. The increase in large pores in those locations with larger surface roughness could provide a motivation for surface roughness measurements as an online process monitoring tool if further testing confirms a relationship.

These observations show that neither the study of individual lines nor individual layers is sufficient to capture the behavior of a printed part. The differences in printing behavior between lines, single layers, and multi-layers, could be explained by a combination of two factors: (1) previously moistened powder alters the flow of binder into the powder and (2) binder in the powder creates cohesive capillary forces that alter the mechanical response of powder to the force of droplets as they impact and infiltrate. High speed X-ray observations during printing of a single lines into loose powder showed significant powder ejection [27], but similar studies have not been done of multi-line or multi-layer printing. This present work suggests that the printing response may be altered significantly when printing next to prior lines or over a previously printed layer.

Effective Saturation

The measured effective saturation of parts as a function of the number of layers is presented in Figure 8. Saturation is consistently lowest in the first layer when the droplets are interacting with dry powder. The increase in effective saturation with subsequent layers indicates that binder is flowing from the printed layer into previously printed layers. It should be noted that in most BJ

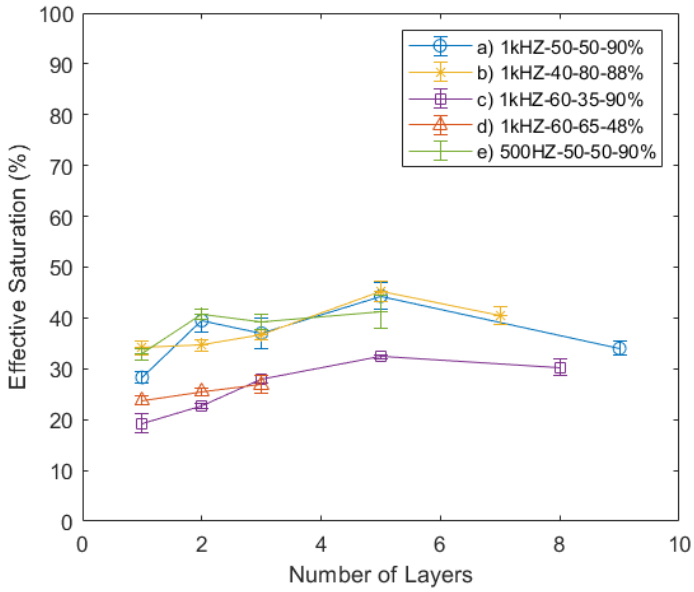

Figure 7: Variation in effective saturation with printing conditions and number of printed layers. Legend depicts print parameters in order: droplet frequency, droplet spacing (µm), layer thickness (µm), and print saturation.

systems print saturation is between 60-80% and sometimes much higher [17]. However, heat is applied to the beds between layers to promote evaporation so that the excess binder beyond the effective saturation measured here can flow into previously printed works. Without drying (as was the case in this work), the mass increases with binder content (Figure 7) creating a natural saturation limit [16]. This phenomenon is reflected in the observation that samples printed with different layer thickness, but similar droplet/line spacing values had similar levels of effective saturation. This implies that binder flowed beyond the target layer thicknesses for at least some print conditions. When effective saturation is smaller than the target print saturation (as observed here), the binder flows beyond the target geometry making the parts thicker and/or wider than expected. Commercial systems often reduce binder saturation in the initial layer(s) to reduce/prevent binder flow beyond the part boundaries.

Like the surface roughness, the effective saturation data falls into two groups that are separated primarily due to droplet spacing. Data groups 'a', 'b', and 'e' (Figure 7) have comparable effective saturation levels for all parts. All have a droplet spacing of 40 or 50 µm. Increasing droplet spacing to 60 µm (data group 'c', Figure 7) reduced effective saturation even though the target print saturation was the same (≈90%) as groups 'a', 'b', and 'e'. The effective saturation of data group 'c', instead, followed closely with that of data group 'd' with the same droplet spacing even though the print saturations of these two groups differs by a factor of nearly two due to different layer thickness values. Droplet spacing has an impact on the effective saturation of the layers just as it had with line printing [19, 30]. The effective saturation of the layers with droplet spacing values of 40 or 50 µm was comparable to the lines printed at comparable velocity with close droplet spacing as seen in Figure 2.

While effective saturation for 40 and 50 µm droplet spacings were comparable, it decreased significantly when printing with 60 µm droplet spacing. Since droplets were 44 µm in diameter, it is probable that the droplets interact with each other during imbibition at droplet spacing values of

50 µm or less. Transitioning from 50 µm to 60 µm droplet spacing, the droplet interaction is expected to decrease significantly. These same parameters also reduced roughness on the first printed layer. Print settings could be optimized to capitalize on this connection. This could be particularly helpful in printing the first layer of a part. These observations could also be used to increase machine productivity. A large value of droplet spacing, and lower saturation would allow for increased printing speeds if part green strength can be maintained. Alternatively, droplet spacing values could be reduced, and layer thickness increased to reduce the total number of layer spreading operations.

While these results show a stable saturation around 20-40% depending on the printing conditions, a standard printing saturation of 70% is used on the ExOne Innovent+ using the same powder. The higher saturation level on the Innovent+ is likely due to the use of drying between layers as seen in prior work [17]. However, the measured layer saturation levels are also significantly below milliliter-scale sessile droplets in the same powder (55-60%) [32]. However, single line saturations for close droplet spacing at the same droplet velocity are comparable to the layer printing results (~35%) (Figure 2), but line printing cannot predict the variation with number of layers and droplet spacing seen in Figure 7. These results show the limitations of using results from simple primitives such as milliliter-scale droplets to predict behavior of 3D parts.

The variation in effective saturation levels with number of layers and droplet/line spacing values makes it challenging to select an ideal saturation value in an unheated powder bed as tested in this work. Under these printing conditions, an ideal saturation would be required that varied with print parameters and layers would be required to achieve accurate geometry. However, drying between layers has been shown to reduce the sensitivity of the part mass to the print saturation in multilayer parts [17].

Impact of Environmental Conditions

Fine powders are becoming more common in printing as they offer improved feature resolution, surface finish, and sintered density. However, the increased surface area of the finer particles also makes them more sensitive to changes in environmental conditions such as ambient humidity [29]. This has largely been viewed as a hindrance in spreading of the powder as high humidity levels decrease flowability [30]. However, ambient humidity may also impact the binder/powder interaction in BJ. The separate impact of powder conditioning and environmental conditions during printing was evaluated through comparison of surface roughness and saturation at four printing conditions which are ambient powder/ambient moisture printing (Amb-Amb), dry powder/80% humidity printing (Dry-80%), dry powder/40% humidity printing (Dry-40%), and dry powder/steamed prior to printing (Dry-Steam).

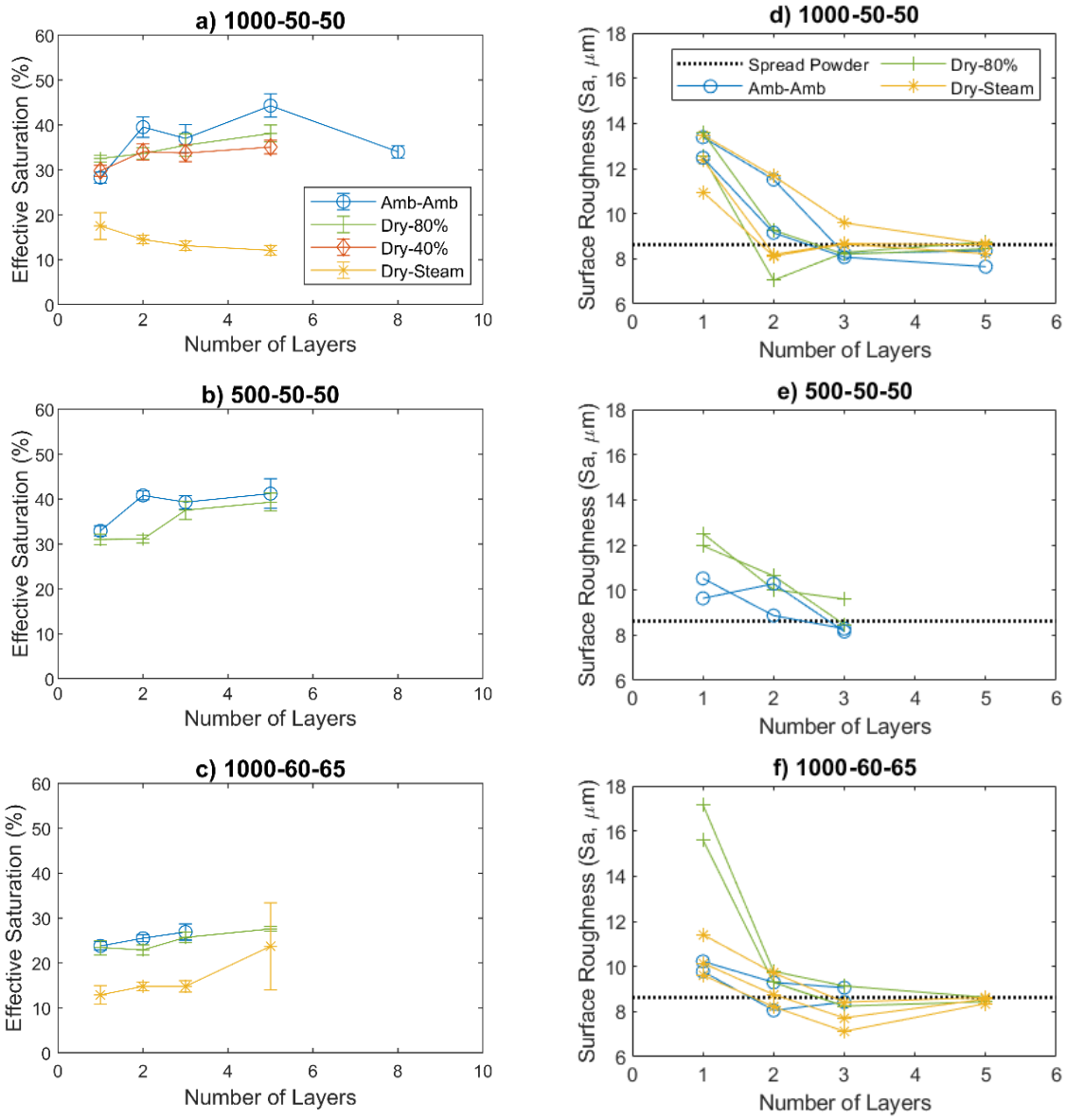

Figure 8: (a, b, c) Saturation values for various printing conditions. (d, e, f) surface roughness values for printing conditions tested. Titles represent droplet frequency (Hz) – droplet spacing (μm) – layer thickness (μm). Ambient moisture (Amb-Amb), dry powder 80% humidity printing (Dry-80%), dry powder 40% humidity printing (Dry-40%), and dry powder steamed printing (Dry-Steam) environments. Each effective saturation data point is an average of six parts. Plots a, b, d, and e had a print saturation at approximately 90%, the plots c and f had a print saturation of 48%.

Effective Saturation

In Figure 9(a, b, c) effective saturation is plotted against number of printed layers for the different environment conditions. Generally, the effective saturation of the dried powders and ambient powders were comparable except at large (60 μm) droplet spacing values (Figure 9c). The humidity exposure during printing was insufficient to impact effective saturation even when exposed for 10 minutes before printing the next layer. This is confirmed by a test in which single

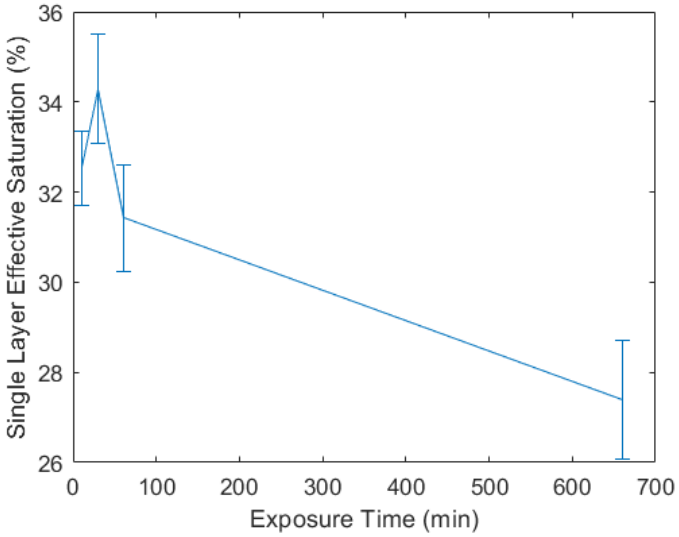

Figure 9: Single layer part effective saturation printed plotted against time exposed for a single layer to 80% humidity prior to printing. Error bars depict the standard deviation of the parts. Layers of powder exposed to humidity <60 minutes exhibited no real change in mass, however prolonged exposure to the ambient humidity significantly changes the imbibition. Error bars depict the standard deviation in the samples.

layers were printed on dry powder exposed to 80% humidity for varying times before printing. Figure 11 shows that for humidity exposures under 60 minutes, there was no significant impact on the effective saturation. It is important to note that most BJ systems will not have powder exposed for prolonged periods of time. Thus, exposure to ambient humidity during printing should have a negligible impact on the effective saturation. Pre-drying powder and dry storage may increase repeatability and predictability of effective saturation. These results show that while humidity control of the powder storage is helpful, humidity control of the printing apparatus itself is probably not necessary for the 316 SS powder studied.

However, this does not mean that moisture does not impact the printing process. The response of the steam-treated powder is very different from the other conditions. In each of the plots in Figure 9(a, b, c) there is a separation between the Dry-Steam and the rest of the conditions. Moisture absorbed into the powder during the steaming treatment significantly increases the flow of the binder in the powder bed—reducing the effective saturation. Due to the lower effective saturation, these parts were significantly larger than the others (Figure 10). It appears that the steam condensed in the powder to create a continuous liquid network in the powder before the binder was printed. During printing, the binder spread quickly along these networks without the constraints of wetting boundaries. These steam-treated parts bled significantly past the intended print volume and resultant parts were fragile due to the low saturation (≈15%).

The low saturation level of the steamed powder could be advantageous to improved printing speed if the green strength were increased and bleeding were controlled. Treating the powder with steam or another liquid source, offers potential advantages such as reduced binder

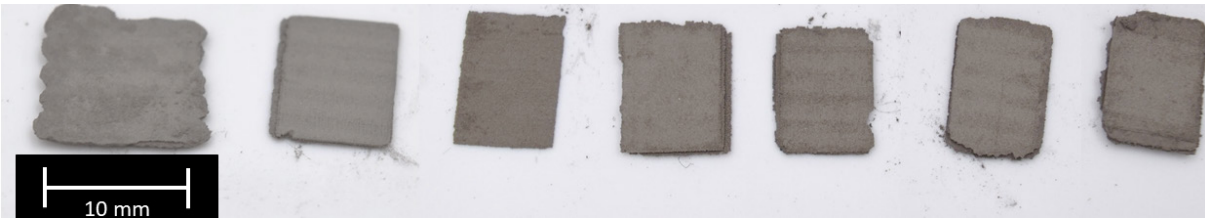

Figure 10: Multilayer parts printed under various conditions. From the left: (1) 3-layHzer part Dry-Steam, 50 µm droplet/line spacing, 1 kHz; (2) 3-layer part Amb-Amb 50 µm droplet/line spacing, 1 k; (3) 1-layer part, Amb-Amb, 50 µm droplet/line 500 Hz; (4) 3-layer part, Amb-Amb 40 µm droplet spacing, line (5) 3-layer part, Amb-Amb 60 µm droplet spacing (6) 5-layer part, Amb-Amb 50 µm droplet spacing (7) 8-layer part, Amb-Amb 50 µm droplet spacing Both parts shown printed at 50 µm droplet/line spacing and 50 µm layer thickness with a droplet velocity of 1000 Hz.

required to fill a desired area and the ability to print thicker layers. This capability can be applied in large area printing and could decrease the number of printing passes or increase the spacing between nozzles on a printhead leading to a significant increase in the printing speed. Pretreatment with moisture could also be used to enhance printing in certain powder/binder combinations that show poor wetting. However, if moisture is added to the powder bed via steam or other methods, steps would be needed to reduce/eliminate bleeding so that accurate part geometry is achieved.

While prior work has shown that droplet frequency has a significant impact on line printing [32], the effective saturation only changed a modest amount from 1000 Hz to 500 Hz in all of the powder environmental conditions. As before, droplet spacing significantly larger than the droplet diameter (60 µm) substantially reduced the effective saturation for all tested conditions as seen in Figure 9(c). At 60 µm droplet spacing, adding additional layers increased the effective saturation of the steamed powder until it was comparable to the other environmental conditions. Reduced sensitivity to moisture in the powder bed could be a helpful characteristic of larger droplet spacings.

Surface Roughness

Figure 9(d, e, f) presents the data for surface roughness values plotted against the number of printed layers. The surface roughness of the as-spread powder at each powder conditioning were approximately equal. The surface roughness decreases with increasing number of layers for all conditions. Additionally, all printing conditions had comparable surface roughness after three printed layers. These measurements show that the interaction between layers becomes the primary driver in determining surface roughness rather than interaction between other droplets in the same layer. Even though the steam treatment dramatically altered the effective saturation levels, the surface roughness of the steamed layers was comparable to Amb-Amb powder conditioning. However, steam treatment does appear to lower the surface roughness compared to Dry-80% at the larger droplet spacing values (60 µm). The combination of Dry-80% powder with large droplet spacing produced the highest surface roughness on the first layer (Figure 9(d, e, f), Figure 6) of any tested condition, but surface roughness was comparable to spread powder layers after printing the second layer.

Linear Regression

Linear regression models were used to analyze the influence of the number of layers, droplet frequency, droplet spacing, and layer thickness on surface roughness and effective saturation for each of the powder conditions. Table 1 summarizes the p-values for effective

saturation. Number of layers was found significant in Amb-Amb and Dry-80%, 40% but not in Dry-Steam. Droplet frequency was insignificant in all cases. Droplet spacing was significant in Amb-Amb and Dry-80%, 40% but insignificant with Dry-Steam. Layer thickness was only significant with Dry-80% and Dry-40% conditioning. Dry-Steam was not influenced by any of the printing parameters. This reduction of sensitivity to printing parameters may help improve printing speed and efficiency if the binder spreading can be controlled to maintain dimensional accuracy.

Table 2 summarizes the linear regression model for surface roughness. As discussed earlier, the number of layers is significant in this regression and is a driving factor in determining surface roughness. Using Amb-Amb powder conditioning, each parameter was found to be significant in determining roughness. This sensitivity to so many parameters is undesirable for process control. However, only droplet spacing influenced the surface roughness of the Dry-80%

Table 2: Effective saturation p-values from linear regression model.

	Number of Layers	Droplet Frequency	Droplet Spacing	Layer Thickness
Amb-Amb	0.017	0.050	0.002	0.518
Dry-80%, 40%	<0.001	0.851	<0.001	<0.001
Dry-Steam	0.510	NA	0.999	0.480

Table 1: Surface roughness p-values from linear regression model.

	Number of Layers	Droplet Frequency	Droplet Spacing	Layer Thickness
Amb-Amb	<0.001	0.013	0.016	0.012
Dry-80%	<0.001	0.965	0.014	0.171
Dry-Steam	0.002	NA	0.999	0.100

powder while Dry-Steam treatment is only sensitive to the number of layers. This implies that the connected network of moisture in the powder changes the imbibition of the binder significantly. There are potential benefits as discussed earlier but the overall outcome may be better controlled if the moisture level were reduced. A controlled partial pre-wetting of the powder in future studies could explore whether there is a regime in which roughness is insensitive to printing parameter variations without loss of dimensional accuracy in the printed parts due to bleeding.

CONCLUSION

While inkjet printing into powder is key to the formation of BJ parts, there is relatively limited understanding of how the droplets and powder interact to form the eventual 3D geometry. Some prior studies have focused on simple primitives such as sessile droplets or individual lines.

This work studied the impact of printing parameters on single- and multi-layer printing by measuring surface roughness and effective saturation as a function of the number of printed layers for the case of no powder-bed heating between layers. Droplet spacing, droplet frequency, and number of printed layers were significant in affecting surface roughness and effective saturation levels under normal printing conditions. Layer thickness was also found to be significant in affecting surface roughness. This work shows that significantly different responses are observed when printing single or multiple layers than single lines or sessile droplets. In many cases, the interaction between previously printed layers and subsequent layers are very significant as seen in the change in roughness and saturation between the first and subsequent printed layers.

Surface roughness was particularly impacted by the number of printed layers. The first printed layer is much rougher than the spread bed and had larger sensitivity to printing parameters, but after 2-4 printed layers, the surface roughness returns to the level of the spread bed. The increased roughness is believed to be caused by powder rearrangement during printing. Powder rearrangement is expected to reduce the density of the green parts and thus, alter shrinkage and sintering results. Cross sections of printed parts show a prevalence of large voids between the first and second layers. This could be caused by the roughness of the printed part, but more data is needed to verify this connection. Surface roughness of all printing conditions eventually converged with increasing layers to approximately the same roughness as the bare powder bed suggesting a less dynamic binder/powder interaction when printing over moist powder. These trends imply that the interaction with the previously printed layer is more significant than the interaction between droplets on the layer being printed. Longer droplet interarrival times (lower printing frequencies) tend to produce less roughness in layers (Figure 8e).Altering process parameters on the first layers for reduced particle rearrangement may be helpful to improve part quality. Parameters such as print speed/droplet frequency and saturation may be altered in subsequent layers to decreasing the overall print time while maintaining part quality.

Effective saturation increased with the number of layers printed for most cases. Droplet spacing and number of layers are significant parameters in determining effective saturation. As droplet spacing increased and layer thickness decreased, effective saturation levels dropped. Ambient humidity levels had no effect on the print quality if the powder was properly conditioned and stored before printing. Parts built with ambient humidity at 40% and 80% show effective saturation was equivalent. However, under long exposure (>60 minutes) the moisture absorbed in the powder from humid air begins to effect saturation levels. Steamed powder had significantly different wetting dynamics as effective saturation levels dropped significantly compared to other powder conditioning and binder spread farther outside the printed volume.

The droplet spacing values (40-60 μm) used in this study to form layers are much larger than could create successful lines in prior work (5-12 μm) [32]. This demonstrates that studies of single lines may not be an effective method for determining print parameters for 3D parts or understanding powder motion during printing. As successive layers are printed, the effects of print parameters become less significant in surface roughness and effective saturation. However, features formed during printing of the first layers may still contribute to porosity and other defects in the final parts near the surface where failure often originates. These results show that special printing parameters should be developed for printing downfacing surfaces to optimize surface quality and minimize porosity. Adjusted print parameters in the powder bulk may be desirable for increased printing speed. Further studies connecting surface roughness to possible defects and identifying methods of controlling binder spread in moist powder will provide greater insight into

strategies for parameter selection and print time reduction. These results show that studies on simple geometries (lines, layers) should be supported by experiments with larger 3D parts.

CRediT AUTHOR STATMENT

Trenton Colton: Investigation, Methodology, Writing-original Draft. **Colton Inkley:** Investigation, Visualization, Writing-Review & Editing. **Adam Berry:** Investigation **Nathan B. Crane:** Conceptualization, Methodology, Resources, Writing – Review & Editing, Supervision, Funding Acquisition

ACKNOWLEDGEMENTS

This work is supported in part by NSF award CMMI-1946724.

REFERENCES

[1] T. Wohlers, R. I. Campbell, R. Huff, O. Diegel, and J. Kowen, *Wohlers report 2019: 3D printing and additive manufacturing state of the industry*: Wohlers Associates, 2019.

[2] W. Du, X. Ren, C. Ma, and Z. Pei, "Binder jetting additive manufacturing of ceramics: A literature review," *ASME International Mechanical Engineering Congress and Exposition, Proceedings (IMECE)*. p. ASME.

[3] P. Nandwana, A. M. Elliott, D. Siddel, A. Merriman, W. H. Peter, and S. S. Babu, "Powder bed binder jet 3D printing of Inconel 718: Densification, microstructural evolution and challenges☆," *Current Opinion in Solid State and Materials Science,* vol. 21, no. 4, pp. 207-218, 2017.

[4] B. M. Wu, S. W. Borland, R. A. Giordano, L. G. Cima, E. M. Sachs, and M. J. Cima, "Solid free-form fabrication of drug delivery devices," *Journal of Controlled Release,* vol. 40, no. 1-2, pp. 77-87, 1996.

[5] L. E. Murr, "Frontiers of 3D Printing/Additive Manufacturing: from Human Organs to Aircraft Fabrication," *Journal of Materials Science & Technology,* vol. 32, no. 10, pp. 987-95, 10/, 2016.

[6] G. Petzow, and W. Huppmann, "Liquid phase sintering," *Zeitschrift fuer Metallkunde,* vol. 67, no. 9, pp. 579-590, 1976.

[7] P. Zovas, R. German, K. Hwang, and C. Li, "Activated and liquid-phase sintering—progress and problems," *JOM,* vol. 35, no. 1, pp. 28-33, 1983.

[8] W. Ji, R. I. Todd, W. Wang, H. Wang, J. Zhang, and Z. Fu, "Transient liquid phase spark plasma sintering of B4C-based ceramics using Ti-Al intermetallics as sintering aid," *Journal of the European Ceramic Society,* vol. 36, no. 10, pp. 2419-2426, 2016.

[9] T. Do, P. Kwon, and C. S. Shin, "Process development toward full-density stainless steel parts with binder jetting printing," *International Journal of Machine Tools and Manufacture,* vol. 121, pp. 50-60, 2017.

[10] J. A. Gonzalez, J. Mireles, Y. Lin, and R. B. Wicker, "Characterization of ceramic components fabricated using binder jetting additive manufacturing technology," *Ceramics International,* vol. 42, no. 9, pp. 10559-64, 07/, 2016.

[11] H. Miyanaji, N. Momenzadeh, and L. Yang, "Effect of powder characteristics on parts fabricated via binder jetting process," *Rapid Prototyping Journal,* vol 25, no 2, pp 332-342, 2018.

[12] M. Ziaee, E. M. Tridas, and N. B. Crane, "Binder-Jet Printing of Fine Stainless Steel Powder with Varied Final Density," *JOM*, pp. 1-5, 2016.

[13] H. Miyanaji, N. Momenzadeh, and L. Yang, "Effect of printing speed on quality of printed parts in Binder Jetting Process," *Additive Manufacturing,* vol. 20, pp. 1-10, 2018.

[14] H. Miyanaji, S. Zhang, A. Lassell, A. Zandinejad, and L. Yang, "Process Development of Porcelain Ceramic Material with Binder Jetting Process for Dental Applications," *JOM,* vol. 68, no. 3, pp. 831-841, 2016/03/01, 2016.

[15] T. Ollison, and K. Berisso, "Three-Dimensional Printing Build Variables That Impact Cylindricity," *Journal of Industrial Technology,* vol. 26, no. 1, 2010.

[16] S. M. Gaytan, M. A. Cadena, H. Karim, D. Delfin, Y. Lin, D. Espalin, E. MacDonald, and R. B. Wicker, "Fabrication of barium titanate by binder jetting additive manufacturing technology," *Ceramics International,* vol. 41, no. 5, pp. 6610-19, 06/, 2015.

[17] N. B. Crane, "Impact of part thickness and drying conditions on saturation limits in binder jet additive manufacturing," *Additive Manufacturing,* vol. 33, pp. 101127, 2020/05/01/, 2020.

[18] H. Miyanaji, M. Orth, J. M. Akbar, and L. Yang, "Process development for green part printing using binder jetting additive manufacturing," *Frontiers of Mechanical Engineering,* vol. 13, no. 4, pp. 504-512, Dec, 2018.

[19] P. R. Baker, "Three dimensional printing with fine metal powders," Massachusetts Institute of Technology, 1997.

[20] K. Lu, and W. T. Reynolds, "3DP process for fine mesh structure printing," *Powder Technology,* vol. 187, no. 1, pp. 11-18, 2008.

[21] M. Ziaee, and N. B. Crane, "Binder Jetting: A Review of Process, Materials, and Methods," *Additive Manufacturing*, 2019/06/22/, 2019.

[22] E. Sachs, M. Cima, P. Williams, D. Brancazio, and J. Cornie, "Three Dimensional Printing: Rapid Tooling and Prototypes Directly from a CAD Model," *Journal of Engineering for Industry,* vol. 114, no. 4, pp. 481-488, 1992.

[23] H. N. Emady, D. Kayrak-Talay, and J. D. Litster, "A regime map for granule formation by drop impact on powder beds," *AIChE Journal,* vol. 59, no. 1, pp. 96-107, 2013.

[24] H. N. Emady, D. Kayrak-Talay, W. C. Schwerin, and J. D. Litster, "Granule formation mechanisms and morphology from single drop impact on powder beds," *Powder Technology,* vol. 212, no. 1, pp. 69-79, 2011.

[25] T. Gao, A. S. S. Singaravelu, S. Oka, R. Ramachandran, F. Štepánek, N. Chawla, and H. N. Emady, "Granule formation and structure from single drop impact on heterogeneous powder beds," *International Journal of Pharmaceutics,* vol. 552, no. 1-2, pp. 56-66, 2018.

[26] J. O. Marston, J. E. Sprittles, Y. Zhu, E. Q. Li, I. U. Vakarelski, and S. T. Thoroddsen, "Drop spreading and penetration into pre-wetted powders," *Powder Technology,* vol. 239, pp. 128-36, 2013.

[27] N. D. Parab, J. E. Barnes, C. Zhao, R. W. Cunningham, K. Fezzaa, A. D. Rollett, and T. Sun, "Real time observation of binder jetting printing process using high-speed X-ray imaging," *Scientific Reports,* vol. 9, no. 1, pp. 2499, 2019/02/21, 2019.

[28] T. Fan, "Droplet-powder impact interaction in three dimentional printing," *MIT Thesis*, 1996.

[29] K. J. Seluga, “Three Dimensional Printing by Vector Printing of Fine Metal Powders,” *Department of Mechanical Engineering, MIT*, 2001.

[30] T. Colton, J. Liechty, A. McLean, and N. B. Crane, “Influence of Drop Velocity and Droplet Spacing on the Equilibrium Saturation Level in Binder Jetting,” *Solid Freeform Fabrication 2019: Proceedings of the 30th Annual International Solid Freeform Fabrication Symposium — An Additive Manufacturing Conference*, pp. 9, 2019, 2019.

[31] M. Lanzetta, and E. Sachs, “Improved surface finish in 3D printing using bimodal powder distribution,” *Rapid Prototyping Journal,* vol. 9, no. 3, pp. 157-66, 2003.

[32] T. Colton, and N. B. Crane, “Influence of droplet velocity, spacing, and inter-arrival time on line formation and saturation in binder jet additive manufacturing,” *Additive Manufacturing*, 2020.

[33] J. Bear, *Modeling phenomena of flow and transport in porous media*: Springer, 2018.

[34] M. T. Stawovy, K. Myers, and S. Ohm, “Binder jet printing of tungsten heavy alloy,” *International Journal of Refractory Metals and Hard Materials,* vol. 83, pp. 104981, 2019/09/01/, 2019.

[35] H. Miyanaji, S. Zhang, and L. Yang, “A new physics-based model for equilibrium saturation determination in binder jetting additive manufacturing process,” *International Journal of Machine Tools and Manufacture,* vol. 124, pp. 1-11, 2018.

[36] Y. Bai, C. Wall, H. Pham, A. Esker, and C. B. Williams, “Characterizing Binder-Powder Interaction in Binder Jetting Additive Manufacturing Via Sessile Drop Goniometry,” *Journal of Manufacturing Science and Engineering-Transactions of the Asme,* vol. 141, no. 1, Jan, 2019.

[37] S. J. Gregorski, “High green density metal parts by vibrational compaction of dry powder in the three-dimensional printing process,” 2003.

[38] S. Cao, Y. Qiu, X. F. Wei, and H. H. Zhang, “Experimental and theoretical investigation on ultra-thin powder layering in three dimensional printing (3DP) by a novel double-smoothing mechanism,” *Journal of Materials Processing Technology,* vol. 220, pp. 231-242, Jun, 2015.

[39] H. Ghadiri, “Crater formation in soils by raindrop impact,” *Earth Surface Processes and Landforms,* vol. 29, no. 1, pp. 77-89, 2004.

[40] M. Ziaee, E. M. Tridas, and N. B. Crane, “Binder-Jet Printing of Fine Stainless Steel Powder with Varied Final Density,” *JOM,* vol. 69, no. 3, pp. 592-596, 2017.

[41] Y. Bai, G. Wagner, and C. B. Williams, “Effect of particle size distribution on powder packing and sintering in binder jetting additive manufacturing of metals,” *Journal of Manufacturing Science and Engineering, Transactions of the ASME,* vol. 139, no. 8, 2017.